

## Supporting Information for

# Luminescence color alteration induced by trapped solvent molecules in crystals of tetrahedral gold(I) complexes: Near-unity luminescence mixed with thermally activated delayed fluorescence and phosphorescence

Masahisa Osawa,<sup>\*a</sup> Hiroto Yamayoshi,<sup>a</sup> Mikio Hoshino,<sup>a</sup> Yuya Tanaka,<sup>b</sup> and Munetaka Akita<sup>b</sup>

<sup>a</sup> Department of Applied Chemistry, Nippon Institute of Technology, Gakuendai 4-1, Miyashiro-Machi, Saitama, 345-8501, Japan

<sup>b</sup> Laboratory for Chemistry and Life Science Institute of Innovative Research, Tokyo Institute of Technology R1-27, 4259 Nagatsuta, Midori-ku, Yokohama 226-8503, Japan

## Contents

Experimental Detail	page
1. General Information	S3–S4
2. NMR Experiments	S5–S6
<b>Fig. S7</b> <sup>1</sup> H NMR spectrum of <b>L<sub>tBu</sub></b> in CD <sub>2</sub> Cl <sub>2</sub> at 293 K.	
<b>Fig. S8</b> <sup>31</sup> P { <sup>1</sup> H} NMR spectrum of <b>L<sub>tBu</sub></b> in CD <sub>2</sub> Cl <sub>2</sub> at 293 K.	
<b>Fig. S9</b> <sup>1</sup> H NMR spectrum of <b>1</b> in CD <sub>2</sub> Cl <sub>2</sub> at 293 K.	
<b>Fig. S10</b> <sup>31</sup> P { <sup>1</sup> H} NMR spectrum of <b>1</b> in CD <sub>2</sub> Cl <sub>2</sub> at 293 K.	
3. Crystal Structure determination	S7–S8
<b>Table S15</b> Crystallographic data for <b>1BG</b> , <b>1OR</b> and <b>1YL</b> .	
<b>Table S16</b> Selected bond distances (Å) and angles (°) for <b>1BG</b> , <b>1OR</b> and <b>1YL</b> .	
4. Thermogravimetric Analyses	S8
<b>Fig. S11</b> TGA data for <b>1BG</b> , <b>1OR</b> , and <b>1YL</b> under argon atmosphere	
5. Photophysical Measurements	S9
<b>Fig. S4</b> Temperature-dependent change of (A) corrected emission spectra and (B) emission lifetime for [Au(L) <sub>2</sub> ]Cl.	
<b>Fig. S5</b> Temperature-dependent change of (A) corrected emission spectra and (B) emission lifetime	

for **1BG**.

**Fig. S6** Temperature-dependent change of (A) corrected emission spectra and (B) emission lifetime for **1OR**.

6. Theoretical Studies

S10–S24

**Fig. S1** The optimized  $S_0$  geometry of  $[\text{Au}(\text{L})_2]^+$  in  $\text{CH}_2\text{Cl}_2$  and the dihedral angle between two planes, P1-Au-P2 and P3-Au-P4.

**Fig. S2** The optimized  $S_0$  geometry of  $\mathbf{1}^+$  in  $\text{CH}_2\text{Cl}_2$  and the dihedral angle between two planes, P1-Au-P2 and P3-Au-P4.

**Fig. S3** The optimized  $T_1$  geometry of  $\mathbf{1}^+$  in  $\text{CH}_2\text{Cl}_2$  and the dihedral angle between two planes, P1-Au-P2 and P3-Au-P4.

**Table S1** The optimized  $T_1$  geometry of  $\mathbf{1}^+$  in  $\text{CH}_2\text{Cl}_2$  and the dihedral angle between two planes, P1-Au-P2 and P3-Au-P4.

**Table S2** Composition of hole and electron for the  $S_0 \rightarrow S_5$  of  $[\text{Au}(\text{L})_2]^+$  in  $\text{CH}_2\text{Cl}_2$ .

**Table S3** Composition of hole and electron for the  $S_0 \rightarrow S_5$  of  $[\text{Au}(\text{L})_2]^+$  in  $\text{CH}_2\text{Cl}_2$ .

**Table S4** Composition of hole and electron for the  $S_0 \rightarrow S_6$  of  $[\text{Au}(\text{L})_2]^+$  in  $\text{CH}_2\text{Cl}_2$ .

**Table S5** Composition of hole and electron for the  $S_0 \rightarrow S_{13}$  of  $[\text{Au}(\text{L})_2]^+$  in  $\text{CH}_2\text{Cl}_2$ .

**Table S6** Composition of hole and electron for the  $S_0 \rightarrow S_{18}$  of  $[\text{Au}(\text{L})_2]^+$  in  $\text{CH}_2\text{Cl}_2$ .

**Table S7** NTO analysis for selected transitions of  $[(\text{L}_{\text{tBu}})_2\text{Au}]^+ \mathbf{1}^+$

**Table S8** Composition of hole and electron for the  $S_0 \rightarrow S_1$  of  $\mathbf{1}^+$  in  $\text{CH}_2\text{Cl}_2$ .

**Table S9** Composition of hole and electron for the  $S_0 \rightarrow S_5$  of  $\mathbf{1}^+$  in  $\text{CH}_2\text{Cl}_2$ .

**Table S10** Composition of hole and electron for the  $S_0 \rightarrow S_6$  of  $\mathbf{1}^+$  in  $\text{CH}_2\text{Cl}_2$ .

**Table S11** Composition of hole and electron for the  $S_0 \rightarrow S_{11}$  of  $\mathbf{1}^+$  in  $\text{CH}_2\text{Cl}_2$ .

**Table S12** Composition of hole and electron for the  $S_0 \rightarrow S_{17}$  of  $\mathbf{1}^+$  in  $\text{CH}_2\text{Cl}_2$ .

**Table S13** NTO analysis for selected transitions of  $\mathbf{1}^+$ .

**Table S14** Composition of hole and electron for the optimized  $T_1$  of  $\mathbf{1}^+$  in  $\text{CH}_2\text{Cl}_2$ .

**Table S17** Results of vertical excited state calculation using atomic coordinates extracted from X-ray crystallographic data

**Table S18** Geometry data of  $[\text{Au}(\text{L})_2]^+$  for the optimized  $S_0$  state in  $\text{CH}_2\text{Cl}_2$ .

**Table S19** Geometry data of  $\mathbf{1}^+$  for the optimized  $S_0$  state in  $\text{CH}_2\text{Cl}_2$

**Table S20** Geometry data of  $\mathbf{1}^+$  for the optimized  $T_1$  state in  $\text{CH}_2\text{Cl}_2$

## 1. General Information

$^1\text{H}$ ,  $^{13}\text{C}$ , and  $^{31}\text{P}$  NMR spectra were recorded on a Bruker AVANCE-400 spectrometer.  $^1\text{H}$  chemical shifts were referenced to residual solvent peaks.  $^{31}\text{P}$  chemical shifts were referenced to an external standard, 85% phosphoric acid ( $\delta = 0$  ppm). Elemental analyses (C and H) were carried out using an elemental analyser (Vario EL CHNOS) from Elementar. For the photo-physical studies, dissolved oxygen was removed by repeated freeze-pump-thaw cycles. Steady-state emission spectra were recorded at room temperature and at 77 K using a Hitachi F-7000 spectrofluorometer. The intensity distribution of the Xenon lamp incorporated in the spectrofluorometer was corrected using Rhodamine B in ethylene glycol. The output of the photomultiplier tube was calibrated between 300 and 850 nm with a secondary standard lamp.

Laser photolysis studies were performed using a Nd:YAG laser (Sure Light 400, Hoya Continuum Ltd.) equipped with second, third, and fourth harmonic generators. The laser pulses used for the emission lifetime measurements were of the third harmonic (355 nm). The duration and energy of the laser pulse were 10 ns and 30 mJ/pulse, respectively. The system used to monitor the emission decay was reported elsewhere.<sup>1</sup>

An Optistat DN-V2 cryostat from Oxford Instruments was used to measure the emission spectra and lifetimes in the temperature range 309–83 K. Crystalline powders of samples used for emission measurements were sealed in quartz tubes with a diameter of 3 mm. Optical measurements at 77 K were carried out at the temperature of liquid nitrogen using a Dewar vessel with four optical windows. After filling the vessel with liquid nitrogen, the sample, which was placed in a quartz tube with a diameter of 5 mm, was immersed into the liquid nitrogen for rapid cooling, and luminescence spectra and lifetimes were measured.

Emission quantum yields were determined at 293 and at 77 K using an absolute PL quantum yield measurement system (C-9920-02G, Hamamatsu).<sup>2</sup>

A suitable crystal for was selected and mounted using Paratone-N oil on a Cryo-Loop. Data collections were performed at 90(2) K on a Bruker APEX-II CCD. The crystallographic data are summarized in Table S1 and S2. Lorentz and polarization corrections and empirical absorption corrections were carried out for data reduction. The structures were solved by direct methods (Shelxs)<sup>3</sup> or charge flipping methods (olex2.solve)<sup>4</sup> and were refined with all non-hydrogen atoms refined anisotropically. Hydrogen atoms were inserted at idealized positions and treated as fixed-atoms. CCDC reference numbers are 1902631 for **1BG**, 1902632 for **1OR** and 1902633 for **1YL**, respectively.

Thermogravimetric analyses (TGA) measurements were performed under argon atmosphere on a Rigaku TG-8120.

The structure in the singlet ground ( $S_0$ ) was optimized by using density functional theory (DFT) and the

triplet excited ( $T_1$ ) structure was optimized using time-dependent (TD)-DFT.<sup>5</sup> The input coordinates were extracted from the X-ray crystallographic data without the anion and crystallization solvents. It was confirmed that crystallization solvent have little influence on the excited states of solvated complexes (Table S17). Vertical excited state calculations were performed to determine  $S_1$  and  $T_1$  energies, and HOMO and (HOMO-1) energies using TD-DFT without geometry optimizations. The B3LYP level of theory<sup>5</sup> were used for all calculations. The LANL2DZ basis set<sup>6</sup> for Au atom, 6-31+G\* basis set for P atoms, and 6-31G\* basis set for C and H atoms, were used. Solvent ( $\text{CH}_2\text{Cl}_2$ ) effects were applied by the integral equation formalism<sup>7</sup> for the polarizable continuum model (PCM)<sup>8</sup> equipped in Gaussian16 B. 01.<sup>9</sup> Natural transition orbitals (NTOs) were generated by orbital transformation followed by a singular value decomposition of the transition density matrix. In the NTO representation, the electronic transitions can be expressed by one single “hole (approximately HOMO) - electron (approximately LUMO)” pair with an associated eigenvalue of essentially one, even for transitions that are highly mixed in the canonical MO basis. This procedure can be a helpful strategy for obtaining a simple orbital interpretation of “what got excited to where”.<sup>10</sup>

## 2. NMR Experiments

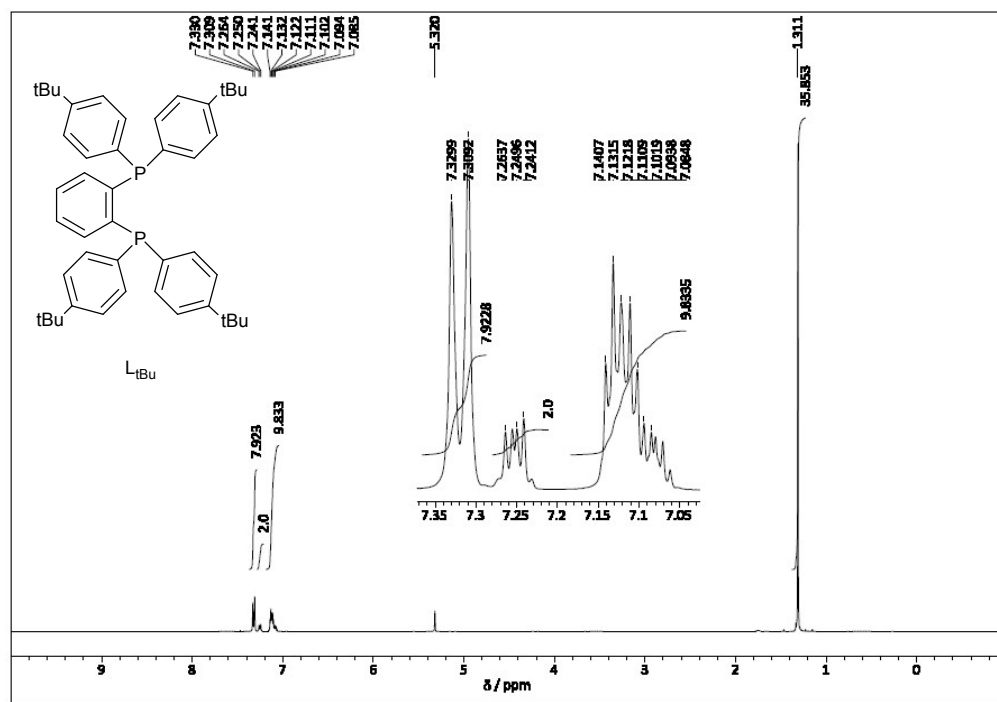


Fig. S7  $^1\text{H}$  NMR spectrum of  $\text{L}_{\text{tBu}}$  in  $\text{CD}_2\text{Cl}_2$  at 293 K.

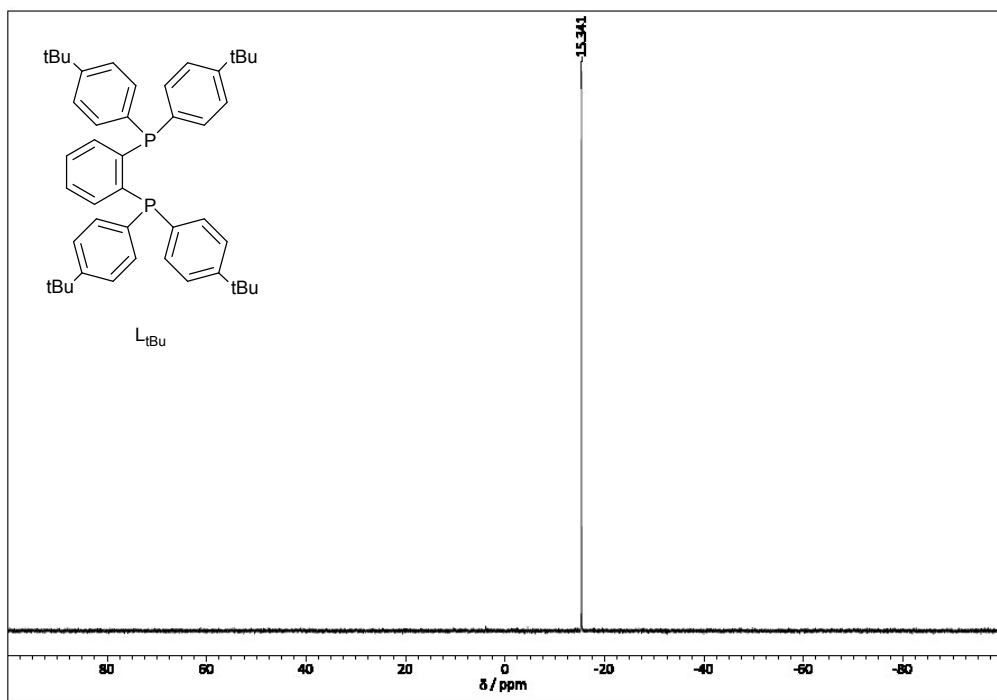


Fig. S8  $^{31}\text{P}$   $\{^1\text{H}\}$  NMR spectrum of  $\text{L}_{\text{tBu}}$  in  $\text{CD}_2\text{Cl}_2$  at 293 K.

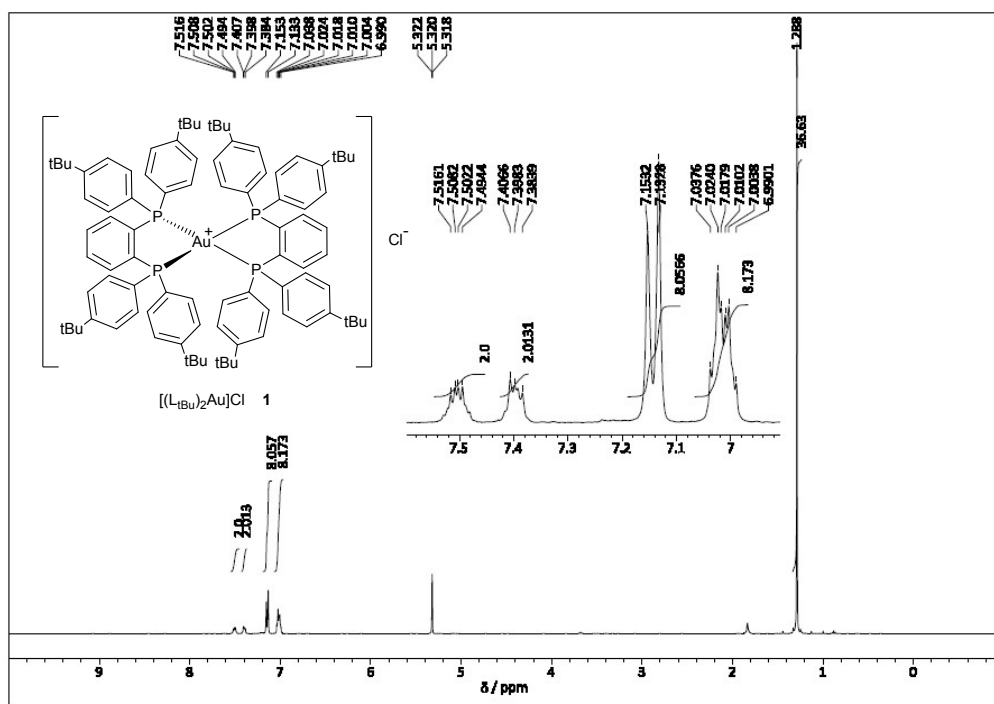


Fig. S9  $^1\text{H}$  NMR spectrum of **1** in  $\text{CD}_2\text{Cl}_2$  at 293 K.

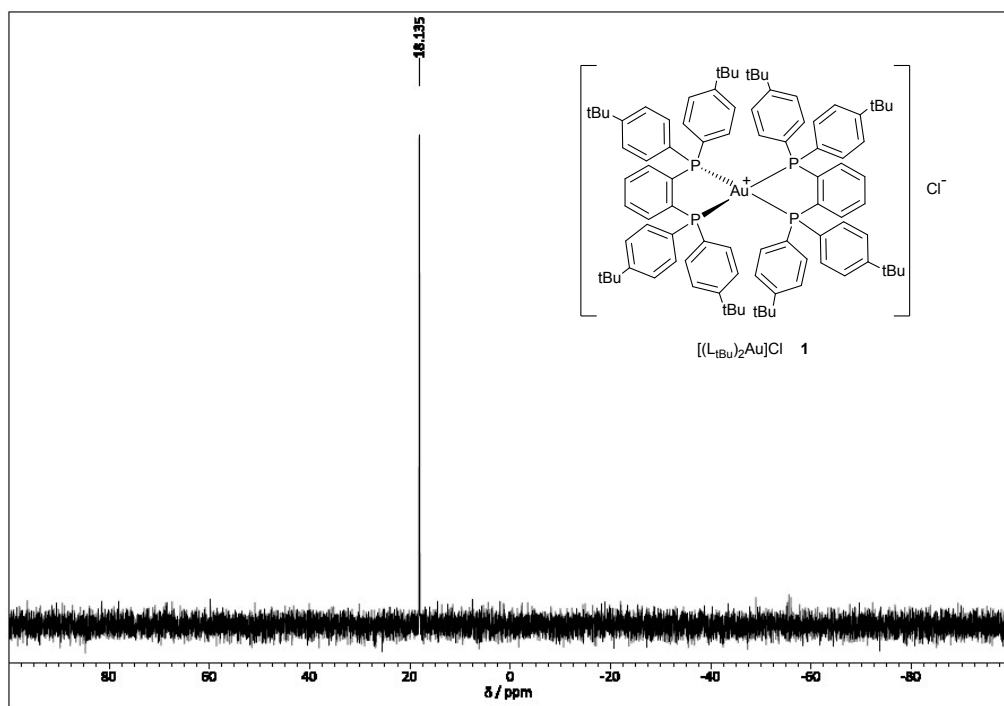


Fig. S10  $^{31}\text{P}$   $\{^1\text{H}\}$  NMR spectrum of **1** in  $\text{CD}_2\text{Cl}_2$  at 293 K.

### 3. Crystal Structure determination

**Table S15.** Crystallographic data for **1BG** and **1OR**.

	<b>1BG</b>	<b>1OR</b>	<b>1YL</b>
formula	C <sub>188</sub> H <sub>232</sub> Au <sub>2</sub> Cl <sub>2</sub> OP <sub>8</sub>	C <sub>99</sub> H <sub>127</sub> Au ClO <sub>2</sub> P <sub>4</sub>	C <sub>187</sub> H <sub>230</sub> Au <sub>2</sub> C <sub>18</sub> O <sub>5</sub> P <sub>8</sub>
formula weight	3220.35	1705.31	3483.02
cryst syst	monoclinic	monoclinic	triclinic
space group	<i>C2/c</i>	<i>P2<sub>1</sub>/n</i>	<i>P</i>
<i>a</i> / Å	44.658(6)	15.4826(19)	15.891(2)
<i>b</i> / Å	17.592(2)	21.679(3)	17.780(3)
<i>c</i> / Å	31.006(5)	27.598(3)	19.707(3)
<i>α</i> / deg	90	90	100.322(2)
<i>β</i> / deg	133.755(3)	90.093(2)	106.859(2)
<i>γ</i> / deg	90	90	111.240(2)
<i>V</i> / Å <sup>3</sup>	17594(4)	9263.4(19)	4707.9(12)
<i>Z</i>	4	4	1
<i>d</i> <sub>calcd</sub> / g cm <sup>-3</sup>	1.216	1.223	1.229
<i>T</i> / K	90(2)	90(2)	90(2)
radiation	Mo Kα (λ = 0.71073 Å)	Mo Kα (λ = 0.71073 Å)	Mo Kα (λ = 0.71073 Å)
μ / cm <sup>-1</sup>	1.818	1.730	1.788
diffractometer	Bruker APEX-II CCD	Bruker APEX-II CCD	Bruker APEX-II CCD
max 2θ / deg	50	50	50
reflns colld	42008	44032	22535
indep reflns	15560 ( <i>R</i> <sub>int</sub> = 0.0182)	16370 ( <i>R</i> <sub>int</sub> = 0.0167)	16621 ( <i>R</i> <sub>int</sub> = 0.0240)
no. of param refined	960	1073	1096
<i>RI</i> , <sup>[a]</sup> <i>wR2</i> ( <i>I</i> > 2σ <i>I</i> ) <sup>[b]</sup>	0.0307, 0.0755	0.0473, 0.1061	0.0631, 0.1443
<i>S</i>	1.064	1.019	1.035

[a]  $RI = \sum ||F_o| - |F_c| | / \sum |F_o|$ . [b]  $wR2 = [\sum w(|F_o| - |F_c|)^2 / \sum w|F_o|^2]^{1/2}$

**Table S16** Selected bond distances (Å) and angles (°) for **1BG**, **1OR** and **1YL**.

	<b>1BG</b>	<b>1OR</b>	<b>1YL</b>
Au1-P1	2.3683(15)	2.3602(12)	2.3751(18)
Au1-P2	2.4025(10)	2.3983(12)	2.3785(16)
Au1-P3	2.4352(12)	2.3719(12)	2.4219(16)
Au1-P4	2.3957(13)	2.4114(12)	2.3736(17)
P1-Au1-P2	86.47(4)	86.58(4)	87.39(6)
P3-Au1-P4	80.66(4)	85.10(4)	82.83(5)

#### 4. Thermogravimetric Analyses

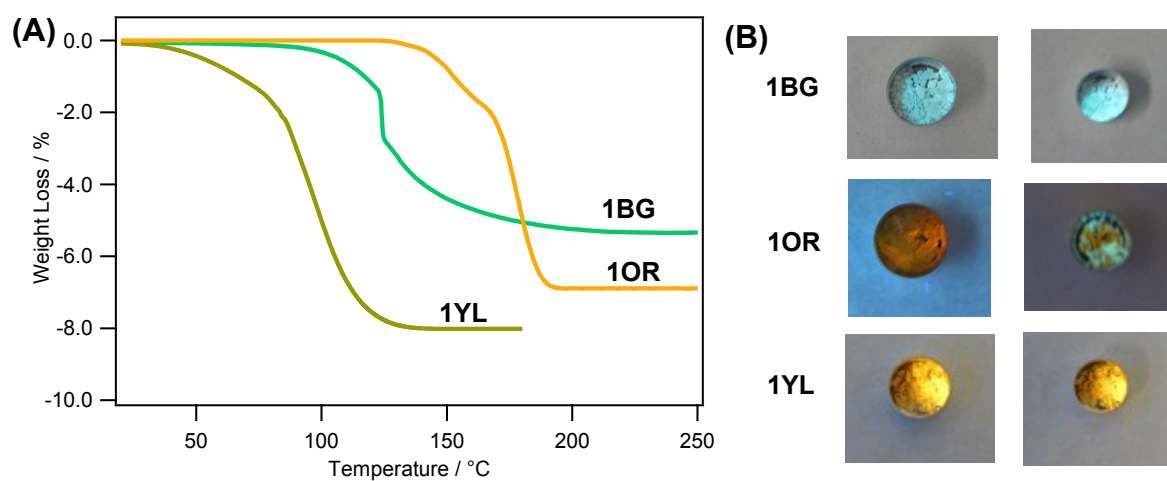


**Fig. S11** (A) TGA data for **1BG**, **1OR**, and **1YL** under argon atmosphere with a heating rate of 15 °C min<sup>-1</sup> for **1BG** and 20 °C min<sup>-1</sup> for **1OR** and **1YL** and (B) luminescence images before (left) and after (right) TGA analyses.



## 5. Photophysical data

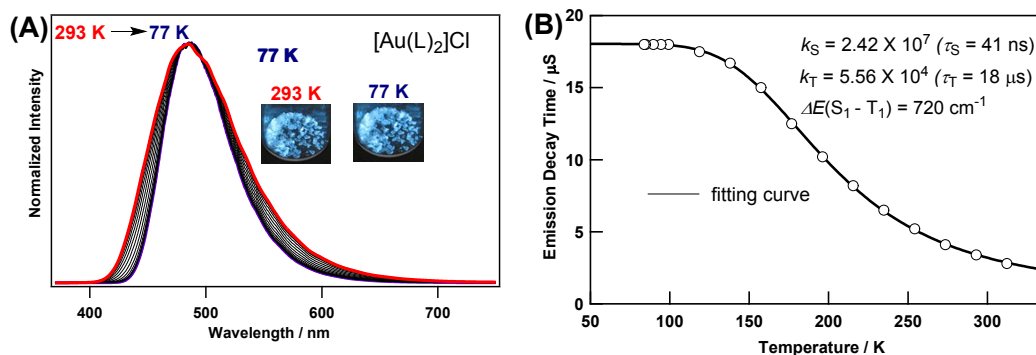


Fig. S4 Temperature-dependent change of (A) corrected emission spectra and (B) emission lifetime for  $[\text{Au}(\text{L})_2]\text{Cl}$ ;  $\lambda_{\text{exc}} = 355 \text{ nm}$ . Inset: Luminescence image of  $[\text{Au}(\text{L})_2]\text{Cl}$  at 293 and 77 K;  $\lambda_{\text{exc}} = 355 \text{ nm}$ .

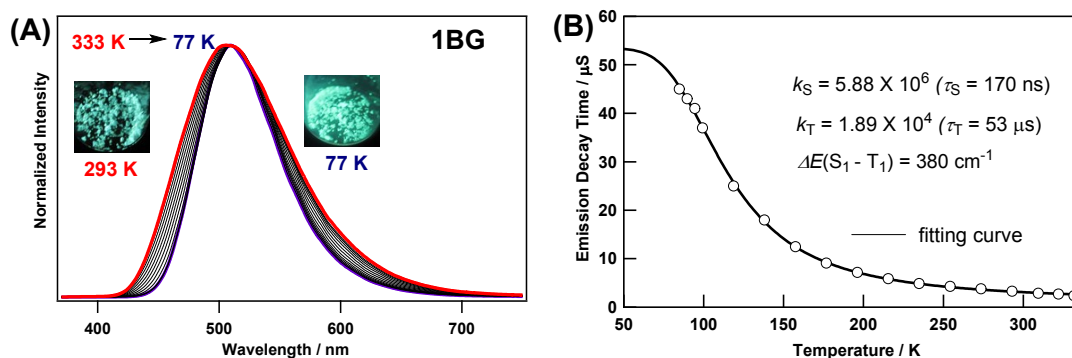


Fig. S5 Temperature-dependent change of (A) corrected emission spectra and (B) emission lifetime for **1BG**;  $\lambda_{\text{exc}} = 355 \text{ nm}$ . Inset: Luminescence image of **1BG** at 293 and 77 K;  $\lambda_{\text{exc}} = 355 \text{ nm}$ .

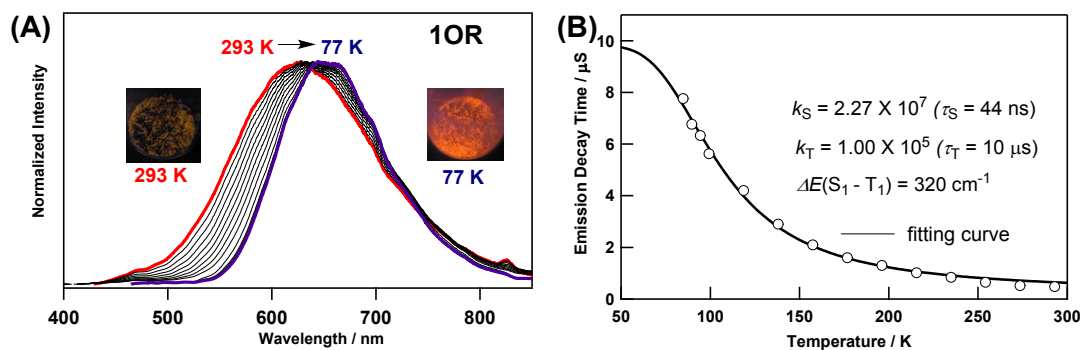
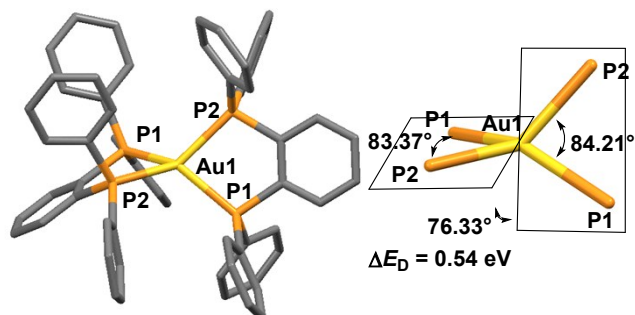
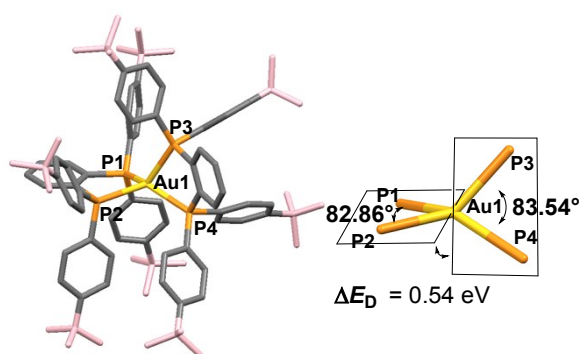


Fig. S6 Temperature-dependent change of (A) corrected emission spectra and (B) emission lifetime for **1OR**;  $\lambda_{\text{exc}} = 355 \text{ nm}$ . Inset: Luminescence image of **1OR** at 293 and 77 K;  $\lambda_{\text{exc}} = 355 \text{ nm}$ .

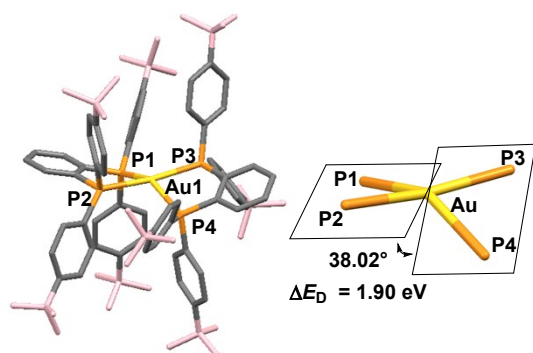
## 6. Theoretical Studies



**Fig. S1** The optimized  $S_0$  geometry of  $[\text{Au}(\text{L})_2]^+$  in  $\text{CH}_2\text{Cl}_2$  and the dihedral angle between two planes, P1-Au-P2 and P3-Au-P4.

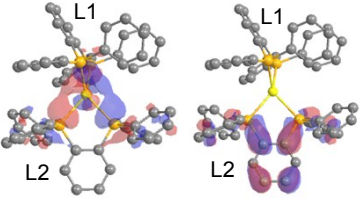
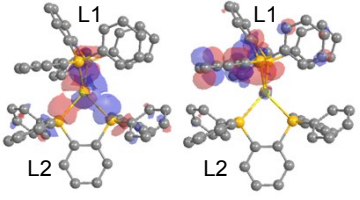
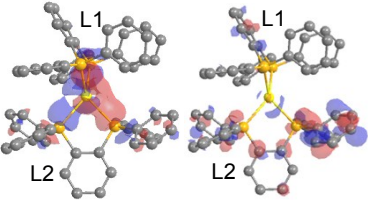
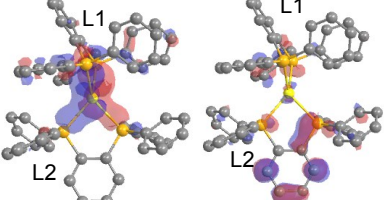
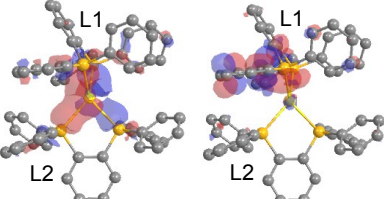


**Fig. S2** The optimized  $S_0$  geometry of  $1^+$  in  $\text{CH}_2\text{Cl}_2$  and the dihedral angle between two planes, P1-Au-P2 and P3-Au-P4.



**Fig. S3** The optimized  $T_1$  geometry of  $1^+$  in  $\text{CH}_2\text{Cl}_2$  and the dihedral angle between two planes, P1-Au-P2 and P3-Au-P4.

**Table S1** NTO analysis for selected transitions of  $[(L)_2Au]^+$ 

states	$\lambda_{cal} /$ nm(eV)	$f$	NTO pairs		Generation probability (%)	Percentage composition (%)
			Hole	Electron		
S <sub>1</sub>	374 (3.320)	0.041		100	$\sigma \rightarrow \pi^*$ : 52 $\pi\pi^*$ : 32 MC+LMCT: 2 Other: 14	
S <sub>5</sub>	330 (3.753)	0.139		98	$\sigma \rightarrow \pi^*$ : 41 $\pi\pi^*$ : 34 MC+LMCT: 11 Other: 14	
S <sub>6</sub>	326 (3.804)	0.141		93	$\sigma \rightarrow \pi^*$ : 42 $\pi\pi^*$ : 31 MC+LMCT: 13 Other: 4	
S <sub>13</sub>	300 (4.139)	0.102		71	$\sigma \rightarrow \pi^*$ : 39 $\pi\pi^*$ : 29 MC+LMCT: 13 Other: 7	
S <sub>18</sub>	289 (4.287)	0.133		95	$\sigma \rightarrow \pi^*$ : 50 $\pi\pi^*$ : 28 MC+LMCT: 12 Other: 10	

**Table S2** Composition of hole and electron for the  $S_0 \rightarrow S_1$  of  $[Au(L)_2]^+$  in  $CH_2Cl_2$ .<sup>a</sup>

percentage composition (%) <sup>b</sup>			
	hole	electron	Difference
Au	29	2	27
P (L1)	13	1	12
P (L2)	27	10	17
phenylene unit (L1)	2	1	1
phenylene unit (L2)	2	57	-55
phenyl groups (L1)	6	0	6
phenyl groups (L2)	22	29	-7

<sup>a</sup> The optimized S<sub>0</sub> geometry was obtained by DFT. <sup>b</sup> The atomic component was evaluated by the Mulliken analysis.

**Table S3** Composition of hole and electron for the S<sub>0</sub> → S<sub>5</sub> of [Au(L)<sub>2</sub>]<sup>+</sup> in CH<sub>2</sub>Cl<sub>2</sub>.<sup>a</sup>

percentage composition (%) <sup>b</sup>			
	hole	electron	Difference
Au	30	11	19
P (L1)	19	12	7
P (L2)	20	2	18
phenylene unit (L1)	3	18	-5
phenylene unit (L2)	2	1	1
phenyl groups (L1)	12	48	-36
phenyl groups (L2)	17	8	9

<sup>a</sup> The optimized S<sub>0</sub> geometry was obtained by DFT. <sup>b</sup> The atomic component was evaluated by the Mulliken analysis.

**Table S4** Composition of hole and electron for the S<sub>0</sub> → S<sub>6</sub> of [Au(L)<sub>2</sub>]<sup>+</sup> in CH<sub>2</sub>Cl<sub>2</sub>.<sup>a</sup>

percentage composition (%) <sup>b</sup>			
	hole	Electron	Difference
Au	29	13	20
P (L1)	18	5	9
P (L2)	22	3	14
phenylene unit (L1)	2	8	-4
phenylene unit (L2)	2	11	-8
phenyl groups (L1)	9	7	3
phenyl groups (L2)	18	53	-33

<sup>a</sup> The optimized S<sub>0</sub> geometry was obtained by DFT. <sup>b</sup> The atomic component was evaluated by the Mulliken analysis.

**Table S5** Composition of hole and electron for the S<sub>0</sub> → S<sub>13</sub> of [Au(L)<sub>2</sub>]<sup>+</sup> in CH<sub>2</sub>Cl<sub>2</sub>.<sup>a</sup>

percentage composition (%) <sup>b</sup>			
	hole	Electron	Difference
Au	27	16	11
P (L1)	24	-2	26
P (L2)	9	10	-1
phenylene unit (L1)	4	3	1
phenylene unit (L2)	2	36	-34
phenyl groups (L1)	23	19	4
phenyl groups (L2)	10	17	-7

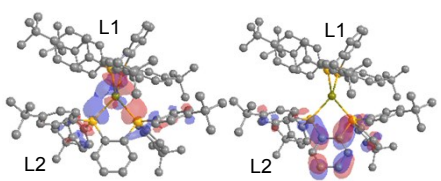
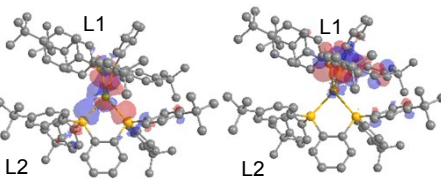
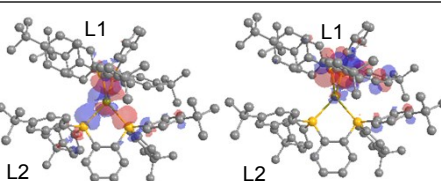
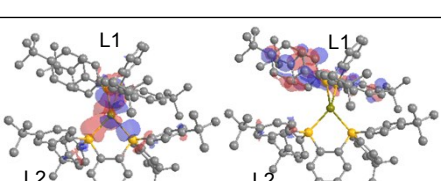
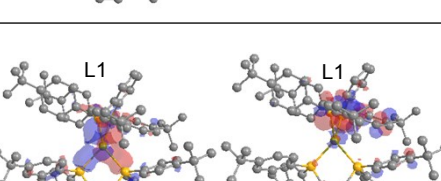
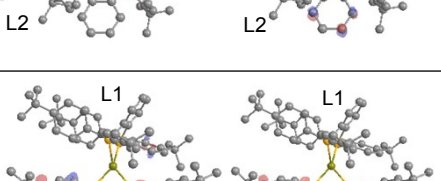
<sup>a</sup> The optimized S<sub>0</sub> geometry was obtained by DFT. <sup>b</sup> The atomic component was evaluated by the Mulliken analysis.

**Table S6** Composition of hole and electron for the S<sub>0</sub> → S<sub>18</sub> of [Au(L)<sub>2</sub>]<sup>+</sup> in CH<sub>2</sub>Cl<sub>2</sub>.<sup>a</sup>

percentage composition (%) <sup>b</sup>			
	hole	Electron	Difference
Au	28	12	12
P (L1)	18	8	10
P (L2)	15	2	13
phenylene unit (L1)	3	6	-3
phenylene unit (L2)	2	1	1
phenyl groups (L1)	20	51	-31
phenyl groups (L2)	14	10	4

<sup>a</sup> The optimized S<sub>0</sub> geometry was obtained by DFT. <sup>b</sup> The atomic component was evaluated by the Mulliken analysis.

**Table S7** NTO analysis for selected transitions of  $[(L_{tBu})_2Au]^+ 1^+$

states	$\lambda_{cal} /$ nm(eV)	$f$	NTO pairs		Generation probability (%)	Percentage composition (%)
			Hole	Electron		
S <sub>1</sub>	377 (3.293)	0.067		100	$\sigma \rightarrow \pi^*$ : 53 $\pi\pi^*$ : 32 MC+LMCT: 2 Other: 13	
S <sub>5</sub>	356 (3.694)	0.195		99	$\sigma \rightarrow \pi^*$ : 41 $\pi\pi^*$ : 34 MC+LMCT: 12 Other: 13	
S <sub>6</sub>	330 (3.757)	0.220		97	$\sigma \rightarrow \pi^*$ : 44 $\pi\pi^*$ : 36 MC+LMCT: 9 Other: 11	
S <sub>11</sub>	309 (4.012)	0.069		85	$\sigma \rightarrow \pi^*$ : 42 $\pi\pi^*$ : 33 MC+LMCT: 12 Other: 13	
S <sub>17</sub>	293 (4.239)	0.232		91	$\sigma \rightarrow \pi^*$ : 34 $\pi\pi^*$ : 39 MC+LMCT: 12 Other: 15	
S <sub>40</sub>	255 (4.867)	0.190		74	$\pi\pi^*$ : 89% Other: 11%	

**Table S8** Composition of hole and electron for the  $S_0 \rightarrow S_1$  of  $\mathbf{1}^+$  in  $\text{CH}_2\text{Cl}_2$ .<sup>a</sup>

	percentage composition (%) <sup>b</sup>		
	hole	electron	Difference
Au	28	2	26
P (L1)	11	0	11
P (L2)	26	10	16
phenylene unit (L1)	2	1	1
phenylene unit (L2)	3	58	-55
phenyl groups (L1)	7	1	6
phenyl groups (L2)	22	19	3

<sup>a</sup> The optimized  $S_0$  geometry was obtained by DFT. <sup>b</sup> The atomic component was evaluated by the Mulliken analysis.

**Table S9** Composition of hole and electron for the  $S_0 \rightarrow S_5$  of  $\mathbf{1}^+$  in  $\text{CH}_2\text{Cl}_2$ .<sup>a</sup>

	percentage composition (%) <sup>b</sup>		
	hole	electron	Difference
Au	29	12	17
P (L1)	17	10	7
P (L2)	20	3	17
phenylene unit (L1)	3	6	-3
phenylene unit (L2)	2	4	-2
phenyl groups (L1)	12	56	-44
phenyl groups (L2)	17	9	8

<sup>a</sup> The optimized  $S_0$  geometry was obtained by DFT. <sup>b</sup> The atomic component was evaluated by the Mulliken analysis.



**Table S10** Composition of hole and electron for the  $S_0 \rightarrow S_6$  of  $\mathbf{1}^+$  in  $\text{CH}_2\text{Cl}_2$ .<sup>a</sup>

percentage composition (%) <sup>b</sup>			
	hole	electron	Difference
Au	29	9	20
P (L1)	15	6	9
P (L2)	21	7	14
phenylene unit (L1)	3	7	-4
phenylene unit (L2)	2	10	-8
phenyl groups (L1)	11	8	3
phenyl groups (L2)	20	53	-33

<sup>a</sup> The optimized  $S_0$  geometry was obtained by DFT. <sup>b</sup> The atomic component was evaluated by the Mulliken analysis.

**Table S11** Composition of hole and electron for the  $S_0 \rightarrow S_{11}$  of  $\mathbf{1}^+$  in  $\text{CH}_2\text{Cl}_2$ .<sup>a</sup>

percentage composition (%) <sup>b</sup>			
	hole	electron	Difference
Au	29	12	17
P (L1)	19	9	10
P (L2)	18	3	15
phenylene unit (L1)	3	4	-1
phenylene unit (L2)	2	1	1
phenyl groups (L1)	13	77	-64
phenyl groups (L2)	16	8	8

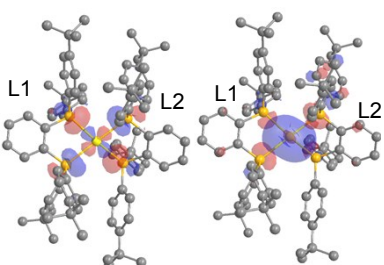
<sup>a</sup> The optimized  $S_0$  geometry was obtained by DFT. <sup>b</sup> The atomic component was evaluated by the Mulliken analysis.

**Table S12** Composition of hole and electron for the  $S_0 \rightarrow S_{17}$  of  $\mathbf{1}^+$  in  $\text{CH}_2\text{Cl}_2$ .<sup>a</sup>

	percentage composition (%) <sup>b</sup>		
	hole	electron	Difference
Au	27	12	15
P (L1)	18	9	9
P (L2)	14	4	10
phenylene unit (L1)	4	6	-2
phenylene unit (L2)	2	9	-7
phenyl groups (L1)	19	51	-32
phenyl groups (L2)	16	9	7

<sup>a</sup> The optimized  $S_0$  geometry was obtained by DFT. <sup>b</sup> The atomic component was evaluated by the Mulliken analysis.

**Table S13** NTO analysis for selected transitions of  $\mathbf{1}^+$ 

states	$\lambda_{\text{cal}} / \text{nm(eV)}$	$f$	NTO pairs		Generation probability (%)	Percentage composition (%)
			Isovalue = 0.035			
			Hole	Electron		
$T_1$	852 (1.460)	0.000			100	MC+LMCT: 53 (MC $\leq$ 25) $\sigma \rightarrow \pi^*$ : 12 $\pi\pi^*$ : 27 Others: 8

**Table S14** Composition of hole and electron for the optimized T<sub>1</sub> of **1**<sup>+</sup> in CH<sub>2</sub>Cl<sub>2</sub>.<sup>a</sup>

	percentage composition (%) <sup>b</sup>		
	hole	Electron	Difference
Au	25	46	-21
P (L1)	24	8	16
P (L2)	24	12	13
phenylene unit (L1)	2	5	-3
phenylene unit (L2)	2	4	-2
phenyl groups (L1)	11	15	-4
phenyl groups (L2)	12	9	-3

<sup>a</sup> The optimized T<sub>1</sub> geometry was obtained by TD-DFT. <sup>b</sup> The atomic component was evaluated by the Mulliken analysis.

**Table S17** Results of vertical excited state calculations using atomic coordinates extracted from X-ray crystallographic data.

	$\square S_1 / \text{nm (eV)}^a$	$T_1 / \text{nm (eV)}^a$	$\Delta E(S_1-T_1) / \text{cm}^{-1} (\text{eV})$	HOMO-(HOMO-1) / eV	HOMO / eV	(HOMO-1) / eV	LUMO / eV
[Au(L) <sub>2</sub> ]Cl	349(3.55)	367(3.38)	1371(0.17)	0.06	-7.58959	-7.65000	-3.34800
<b>1BG</b>	361(3.45)	377(3.29)	1130(0.14)	0.39	-7.05814	-7.45162	-2.95931
<b>1OR</b>	394(3.15)	410(3.03)	968(0.12)	0.73	-6.79147	-7.52101	-2.99495
<b>1OR</b> <sup>b</sup>	394(3.15)	410(3.03)	956(0.12)	0.73	-6.81035	-7.54942	-3.02978
<b>1YL</b>	369(3.36)	384(3.23)	1080(0.13)	0.42	-7.02794	-7.34087	-2.97338

<sup>a</sup> Vertical (Franck-Condon) excited states. <sup>b</sup> Calculation results including crystallization solvents (THF and *n*-hexane).

**Table S18** Geometry data of  $[\text{Au}(\text{L})_2]^+$  for the optimized  $S_0$  state in  $\text{CH}_2\text{Cl}_2$

Au	-0.078704	-0.126130	-0.110725
P	-0.075565	0.052358	2.967185
P	2.150280	-0.038701	0.400337
Cl	-2.298020	-0.199193	-0.907157
C	2.513045	-0.753231	2.058036
C	1.331383	2.051973	4.412936
C	3.924919	-2.867228	-2.027642
C	3.856816	3.447093	1.727810
C	3.406436	2.137195	1.608937
C	1.590956	-0.730820	3.131532
C	3.037254	-2.279109	-1.119054
C	3.760967	-1.368110	2.235150
C	0.194305	1.744399	3.650824
C	-0.755214	2.755364	3.383509
C	5.024226	-2.184901	-2.535853
C	2.768209	1.691337	0.443274
C	3.277152	-0.940724	-0.738419
C	-2.032759	2.499770	2.604549
C	1.930595	2.192986	-1.957645
C	4.398200	-0.263556	-1.240187
C	0.910505	-3.501062	-1.692518
C	1.956033	-1.357805	4.331469
C	0.601886	2.931553	-2.146057
C	1.892815	-3.119161	-0.581762
C	2.856723	2.431453	-3.154793
C	-0.516100	4.039085	3.889032
C	-2.137275	3.399363	1.370930
C	0.617434	4.335015	4.637101
C	4.105096	-1.971218	3.440083
C	-1.570310	-2.074875	4.080097
C	-1.049188	-0.780185	4.297375
C	3.671382	4.330190	0.670143
C	3.194057	-1.972104	4.491117
C	2.410583	-4.358994	0.154408
C	5.270324	-0.876496	-2.132711
C	3.047030	3.891892	-0.492231
C	1.548007	3.334540	4.903736
C	2.586214	2.579180	-0.642357
C	-3.267934	2.643615	3.499547
C	-1.295451	-2.873818	2.818753
C	-1.351692	-0.108704	5.491690
C	-2.152001	-0.693899	6.467646
C	-2.367430	-2.645416	5.078933
C	-2.661582	-1.972046	6.259503
C	-0.503964	-4.148455	3.126178
C	-2.588389	-3.193452	2.063827
H	2.057858	1.274351	4.630334
H	3.752033	-3.893710	-2.340780
H	4.342508	3.770811	2.643657
H	3.551813	1.453473	2.438307
H	4.471731	-1.383725	1.414210
H	5.690142	-2.678337	-3.238448

H	-2.008421	1.463508	2.244043
H	1.705268	1.119556	-1.935170
H	4.592597	0.757700	-0.927956
H	0.504736	-2.610595	-2.184928
H	0.071563	-4.070426	-1.276491
H	1.393470	-4.122946	-2.455258
H	1.251994	-1.360017	5.158821
H	0.756063	4.015616	-2.200414
H	-0.087569	2.725981	-1.320229
H	0.118988	2.611687	-3TGA.076243
H	1.335344	-2.521820	0.150300
H	2.369611	2.088246	-4.074319
H	3.801250	1.888169	-3.049204
H	3.088279	3.495296	-3.280415
H	-1.240382	4.826200	3.693338
H	-2.222232	4.456837	1.648545
H	-3.024426	3.134779	0.784666
H	-1.258793	3.288742	0.726241
H	0.770793	5.342960	5.013595
H	5.077268	-2.443038	3.549581
H	4.013552	5.358703	0.745675
H	3.444535	-2.445176	5.436571
H	2.954799	-5.029868	-0.520138
H	1.571435	-4.922971	0.576482
H	3.082690	-4.083596	0.974337
H	6.131731	-0.332004	-2.508759
H	2.913958	4.591361	-1.313488
H	2.436489	3.548162	5.491950
H	-3.215448	1.968948	4.361067
H	-4.175527	2.403924	2.933757
H	-3.368509	3.668586	3.876653
H	-0.679568	-2.258233	2.149449
H	-0.953987	0.887732	5.659884
H	-2.371522	-0.153346	7.384474
H	-2.771681	-3.643346	4.925935
H	-3.287447	-2.444377	7.012035
H	0.446324	-3.918498	3.620379
H	-0.285030	-4.692089	2.199916
H	-1.071383	-4.821477	3.779856
H	-3.251049	-3.834318	2.657395
H	-2.361982	-3.720660	1.129906
H	-3.134355	-2.278332	1.811940

**Table S19** Geometry data of  $\text{I}^+$  for the optimized  $S_0$  state in  $\text{CH}_2\text{Cl}_2$

Au	0.270929	-0.126094	0.290424
I	-0.187192	-0.243471	2.889341
P	1.053110	-0.021096	-1.889437
P	-2.279445	0.077316	-1.308690
C	0.311613	-1.307082	-4.245061
C	-2.415237	-1.295810	-3.773840
C	-4.023744	-2.057193	-0.656738
C	3.613649	-0.262344	-2.976821
C	-5.103018	-0.037999	-1.471234

C	-3.928575	-0.742246	-1.164342	H	4.743349	3.422695	-0.746438
C	-1.917379	-1.892853	-4.927701	H	2.635964	3.967521	0.714142
C	-1.570743	-0.687077	-2.834632	H	3.027302	2.538027	1.687312
C	-2.820023	2.090186	-3.232773	H	1.417736	2.701081	0.966949
C	-0.176292	-0.708406	-3.074593	H	-7.427827	-2.367956	-0.646427
C	2.986952	2.154058	-0.447494	H	0.838817	-2.500747	-1.050760
C	4.822913	-0.883038	-3.268403	H	1.007504	-4.060017	-2.976468
C	-2.715070	1.781295	-1.867738	H	0.577782	-4.901148	-1.474507
C	-0.547324	-1.892818	-5.168755	H	2.224410	-5.015358	-2.109418
C	-5.297326	-2.612238	-0.487778	H	0.307549	3.857530	-4.851645
C	5.035213	-2.192408	-2.849126	H	3.100767	-4.116690	0.224792
C	1.358114	1.713231	-2.413775	H	1.412417	-4.059241	0.759952
C	-6.358333	-0.608949	-1.288392	H	2.418747	-2.603141	0.854545
C	-2.942845	2.793029	-0.908790	H	-2.828923	-2.394962	1.819896
C	2.204191	2.576224	-1.679596	H	-1.899772	-3.849274	1.421728
C	0.693455	2.191061	-3.551801	H	-3.669846	-3.910807	1.431993
C	-2.809946	-2.896843	-0.301244	H	2.973585	4.577060	-1.573072
C	2.603821	-0.932381	-2.270351	H	-3.212433	3.586856	-4.725758
C	2.800241	-2.271194	-1.867636	H	-3.450466	4.864429	-0.640083
C	4.031699	-2.867357	-2.164047	H	-3.615184	5.381435	-3.038646
C	4.494673	2.362137	-0.625062	H	-0.911216	3.426866	0.840613
C	2.484457	2.885157	0.801022	H	-1.821766	3.221786	2.347216
C	-6.455272	-1.906045	-0.794222	H	-2.241628	4.531776	1.232234
C	1.748527	-3.104600	-1.158471	H	1.784336	5.400977	-3.559669
C	1.370579	-4.340119	-1.981641	H	-3.571667	-4.798396	-1.055816
C	0.838491	3.508777	-3.970721	H	-1.807671	-4.709501	-0.949825
C	2.200527	-3.491700	0.252187	H	-2.660939	-3.861962	-2.255008
C	-2.806848	-3.283246	1.179997	H	-4.700659	3.643609	1.107586
C	2.329788	3.896915	-2.124780	H	-4.233035	2.404137	2.285303
C	-3.137797	3.373095	-3.662884	H	-4.978224	1.929103	0.746882
C	-3.266403	4.076809	-1.366636	H	-2.519735	1.522741	0.750883
C	-3.362801	4.373206	-2.720833				
C	-1.909093	3.488427	1.288244				
C	1.660467	4.367151	-3.249037				
C	-2.708935	-4.136344	-1.195603				
C	-4.283431	2.634886	1.215036				
C	-2.888292	2.543721	0.587634				
H	1.381229	-1.322998	-4.432443				
H	-3.486773	-1.297962	-3.594599				
H	3.451808	0.759985	-3.303984				
H	-5.033909	0.973458	-1.860030				
H	-2.600965	-2.352532	-5.636078				
H	-2.654029	1.312781	-3.972755				
H	2.827305	1.081455	-0.281395				
H	5.590409	-0.343893	-3.816346				
H	-0.143501	-2.351943	-6.066484				
H	-5.384056	-3.625468	-0.102488				
H	5.976647	-2.691903	-3.060806				
H	-7.252252	-0.042050	-1.534254				
H	0.048655	1.526690	-4.117271				
H	-1.910110	-2.291782	-0.475207				
H	4.205650	-3.894409	-1.853335				
H	4.877503	1.821263	-1.496384				
H	5.026360	1.996927	0.260714				
Table S20 Geometry data of $\text{I}^+$ for the optimized $T_1$ state in $\text{CH}_2\text{Cl}_2$							
Au	-0.042222	-0.009961	0.155439				
P	-0.080756	2.517752	0.064097				
P	-2.595207	0.353502	0.050322				
P	2.464768	-0.453964	0.606597				
P	0.243643	-2.114686	-1.205918				
C	0.125660	3.261776	-1.611463				
C	1.062947	3.445913	1.150345				
C	0.496050	-1.873859	-3.008193				
C	-3.428319	-0.628741	1.365641				
C	-0.560763	-1.368205	-3.785542				
C	2.028265	-4.274226	-0.951031				
C	2.298120	3.901704	0.668500				
C	-2.718030	-0.912916	2.544868				
C	5.165765	0.566843	0.624835				
C	-0.389143	-1.112327	-5.146625				
C	-3.644473	0.186583	-1.442068				
C	2.313745	-1.587995	3.187054				
C	-1.632617	-3.610419	0.209667				
C	2.648234	-0.450460	2.430329				
C	3.946551	0.423407	-0.059546				
C	0.769167	3.643477	2.511320				

C -1.771321 3.031732 0.597862  
 C 1.737390 -2.076632 -3.637132  
 C -2.443942 -5.185520 -1.925547  
 C -1.472436 -4.205669 -2.119425  
 C 1.784922 -2.931697 -0.618441  
 C -4.761986 -1.050317 1.281918  
 C 3.217288 -4.898994 -0.569293  
 C -3.946152 1.294965 -2.260362  
 C -4.113225 2.519282 0.988321  
 C 2.703474 -0.385084 5.281307  
 C -4.967047 -0.144821 -3.959790  
 C 2.894645 4.806595 2.860561  
 C 3.936994 -2.854933 0.498971  
 C 1.896331 -1.811237 -4.995776  
 C -1.053728 -3.398945 -1.048953  
 C -3.994845 -1.090699 -1.922912  
 C -5.358704 -1.747151 2.336458  
 C 0.323813 4.323929 -4.247953  
 C 0.840375 -1.329370 -5.790190  
 C 3.018629 0.746620 4.515985  
 C 0.189067 4.646308 -1.827921  
 C -2.024523 4.359411 0.979172  
 C 1.664300 4.317365 3.338170  
 C 3.841912 0.970972 -1.345619  
 C 2.348490 -1.551411 4.578152  
 C -4.593958 1.126161 -3.479950  
 C -4.658542 -2.042162 3.515488  
 C -3.034022 -5.409068 -0.668083  
 C -2.831134 2.102256 0.592379  
 C 3.192601 4.568118 1.510618  
 C -4.648373 -1.244178 -3.146919  
 C 6.236460 1.227948 0.027656  
 C -4.352303 3.842156 1.363785  
 C -3.323540 -1.602242 3.591854  
 C 4.176167 -4.185425 0.150074  
 C -3.306643 4.764697 1.356563  
 C 2.988814 0.722207 3.118730  
 C 2.741791 -2.216697 0.128154  
 C -2.600762 -4.599391 0.393563  
 C -5.687343 -0.278973 -5.311632  
 C 0.168386 2.414473 -2.728651  
 C 0.284913 5.161750 -3.121583  
 C 6.147399 1.771634 -1.267679  
 C 0.431888 4.863657 -5.684579  
 C -6.010982 -1.744360 -5.659917  
 C 4.924595 1.624234 -1.939010  
 C 1.052628 -1.089170 -7.294660  
 C 0.265836 2.938525 -4.016962  
 C -7.017207 0.512449 -5.264991  
 C -4.103766 -6.501954 -0.502532  
 C -5.288759 -2.801808 4.695363  
 C 1.320833 -0.741770 7.354726  
 C 2.730277 -0.391187 6.819150  
 C 5.136398 6.015386 3.098581  
 C 3.836015 5.579621 3.800426  
 C 7.358268 2.493348 -1.883576  
 C -4.790232 0.298164 -6.433391

C -6.749348 -3.206456 4.419163  
 C 3.142824 0.973014 7.403970  
 C 8.551140 1.510191 -1.966698  
 C 7.746987 3.696573 -0.990586  
 C 3.109872 6.848791 4.309616  
 C 4.214338 4.689449 5.008155  
 C -0.775815 4.363699 -6.513638  
 C 0.444580 6.403555 -5.733819  
 C 7.067593 3.019762 -3.301944  
 C -3.493467 -7.874473 -0.877033  
 C 3.743560 -1.453821 7.309637  
 C -4.635400 -6.587495 0.941037  
 C 1.743291 4.347872 -6.324765  
 C -5.297017 -6.198511 -1.440665  
 C -4.474084 -4.088668 4.971847  
 C -0.190929 -0.482240 -7.972001  
 C -5.264839 -1.900740 5.953941  
 C 2.240452 -0.121570 -7.510999  
 C 1.368240 -2.442486 -7.978083  
 H -1.532039 -1.180017 -3.335639  
 H 1.287187 -4.833107 -1.514246  
 H 2.572584 3.748208 -0.370183  
 H -1.680341 -0.596684 2.634245  
 H 5.285695 0.166870 1.626852  
 H -1.240437 -0.738120 -5.704189  
 H 2.027711 -2.510577 2.691624  
 H -1.337041 -2.990814 1.051954  
 H -0.167895 3.286889 2.928341  
 H 2.583886 -2.453580 -3.072601  
 H -2.741702 -5.788378 -2.778498  
 H -1.044952 -4.070540 -3.107785  
 H -5.348073 -0.843590 0.392384  
 H 3.391217 -5.937174 -0.836446  
 H -3.683080 2.298310 -1.939391  
 H -4.929732 1.804075 1.005603  
 H 4.684743 -2.313523 1.069878  
 H 2.868642 -1.998367 -5.442295  
 H -3.763059 -1.977783 -1.340585  
 H -6.391641 -2.055939 2.222109  
 H 3.293178 1.675729 5.001329  
 H 0.170265 5.337662 -0.991058  
 H -1.216210 5.082788 0.995923  
 H 1.388250 4.467577 4.377662  
 H 2.904385 0.893759 -1.891061  
 H 2.092088 -2.455981 5.121913  
 H -4.817914 2.012530 -4.066813  
 H 4.130002 4.910546 1.087641  
 H -4.908149 -2.249376 -3.460107  
 H 7.162677 1.315598 0.588437  
 H -5.350930 4.145774 1.664244  
 H -2.738052 -1.798485 4.485686  
 H 5.106093 -4.661439 0.447148  
 H -3.480723 5.795737 1.650105  
 H 3.230488 1.629974 2.574378  
 H -3.022791 -4.721535 1.384305  
 H 0.120993 1.337065 -2.593645  
 H 0.329740 6.238475 -3.239193

H	-5.104405	-2.355480	-5.737659	H	-6.064121	-6.975031	-1.336902
H	-6.672115	-2.204343	-4.916616	H	-5.754945	-5.233695	-1.193327
H	-6.522170	-1.786659	-6.628074	H	-4.484374	-4.754280	4.100605
H	4.795487	2.026924	-2.937176	H	-3.429688	-3.867332	5.215511
H	0.296250	2.243724	-4.851012	H	-4.906266	-4.633634	5.819572
H	-6.852105	1.576036	-5.062954	H	-0.461905	0.485915	-7.534472
H	-7.539154	0.432271	-6.226130	H	0.014586	-0.319313	-9.035660
H	-7.679576	0.119779	-4.484787	H	-1.060724	-1.145326	-7.902873
H	0.582285	0.000323	7.029578	H	-5.841292	-0.982921	5.790079
H	0.985317	-1.725364	7.009519	H	-5.705990	-2.431739	6.805910
H	1.327089	-0.757255	8.451139	H	-4.245159	-1.613578	6.231157
H	4.940599	6.686036	2.254272	H	2.047362	0.849861	-7.041032
H	5.771436	6.556073	3.808861	H	3.173943	-0.516237	-7.097001
H	5.709130	5.156578	2.730119	H	2.397662	0.046507	-8.582958
H	-4.552301	1.353533	-6.263834	H	0.538489	-3.147720	-7.852890
H	-3.845253	-0.253982	-6.502547	H	2.270003	-2.905077	-7.562916
H	-5.298708	0.221722	-7.402047	H	1.530441	-2.295271	-9.052576
H	-6.831940	-3.869499	3.550297				
H	-7.149751	-3.745011	5.285118				
H	-7.390094	-2.334057	4.247495				
H	4.148676	1.267593	7.083585				
H	2.444688	1.768243	7.118548				
H	3.148337	0.915228	8.498030				
H	8.306904	0.650057	-2.600774				
H	9.424502	2.013463	-2.398235				
H	8.838453	1.131260	-0.980320				
H	8.011777	3.383689	0.024851				
H	8.613131	4.217190	-1.416084				
H	6.921433	4.414371	-0.918585				
H	2.195726	6.602093	4.859794				
H	3.764809	7.412668	4.984455				
H	2.835778	7.504927	3.475428				
H	3.333185	4.372819	5.576234				
H	4.749232	3.790512	4.679913				
H	4.869697	5.241434	5.692218				
H	-1.719996	4.718616	-6.084632				
H	-0.707184	4.739134	-7.541435				
H	-0.816580	3.270312	-6.560737				
H	1.302071	6.823436	-5.195802				
H	0.515179	6.734721	-6.775661				
H	-0.470872	6.832977	-5.311110				
H	6.812128	2.209457	-3.994218				
H	6.248429	3.747906	-3.307980				
H	7.958471	3.521753	-3.694998				
H	-3.135728	-7.893809	-1.911844				
H	-2.648898	-8.119961	-0.222854				
H	-4.247260	-8.663403	-0.769450				
H	4.754409	-1.226496	6.951649				
H	3.767840	-1.473524	8.405732				
H	3.481648	-2.459267	6.963786				
H	-3.841245	-6.833302	1.655241				
H	-5.106063	-5.650004	1.259107				
H	-5.392805	-7.376380	1.005227				
H	2.617862	4.694995	-5.762476				
H	1.777219	3.253731	-6.359219				
H	1.831623	4.717675	-7.353155				
H	-4.993477	-6.168885	-2.492370				



## References

1. M. Hoshino, H. Sonoki, Y. Miyazaki, Y. Iimura and K. Yamamoto, *Inorg. Chem.*, 2000, **39**, 4850-4857.
2. M. Osawa, I. Kawata, S. Igawa, M. Hoshino, T. Fukunaga and D. Hashizume, *Chem. - Eur. J.*, 2010, 12114-12126.
3. G. M. Sheldrick *Acta Cryst.*, 2008, *A64*, 112-122.
4. O. V. Dolomanov, L. J. Bourhis, R. J. Gildea, J. A. K. Howard and H. Puschmann. *J. Appl. Cryst.* 2009, **42**, 339- 341.
5. (a) C. Adamo and V. Barone, *J. Chem. Phys.*, 1999, **110**, 6158-6170; (b) J. P. Perdew, M. Ernzerhof and K. Burke, *J. Chem. Phys.*, 1996, **105**, 9982-9985.
6. (a) P. J. Hay, W. R. Wadt, *J. Chem. Phys.*, 1985, **82**, 270-283; (b) P. J. Hay, W. R. Wadt, *J. Chem. Phys.*, 1985, **82**, 299-310.
7. (a) E. Cancès, B. Mennucci and J. Tomasi, *J. Chem. Phys.*, 1997, **107**, 3032-3041; (b) B. Mennucci, E. Cancès and J. Tomasi, *J. Phys. Chem. B*, 1997, **101**, 10506-10517.
8. S. Miertus, E. Scrocco and J. Tomasi, *Chem. Phys.*, 1981, **55**, 117-129.
9. Gaussian 16, Revision B.01, M. J. Frisch, G. W. Trucks, H. B. Schlegel, G. E. Scuseria, M. A. Robb, J. R. Cheeseman, G. Scalmani, V. Barone, G. A. Petersson, H. Nakatsuji, X. Li, M. Caricato, A. V. Marenich, J. Bloino, B. G. Janesko, R. Gomperts, B. Mennucci, H. P. Hratchian, J. V. Ortiz, A. F. Izmaylov, J. L. Sonnenberg, D. Williams-Young, F. Ding, F. Lipparini, F. Egidi, J. Goings, B. Peng, A. Petrone, T. Henderson, D. Ranasinghe, V. G. Zakrzewski, J. Gao, N. Rega, G. Zheng, W. Liang, M. Hada, M. Ehara, K. Toyota, R. Fukuda, J. Hasegawa, M. Ishida, T. Nakajima, Y. Honda, O. Kitao, H. Nakai, T. Vreven, K. Throssell, J. A. Montgomery, Jr., J. E. Peralta, F. Ogliaro, M. J. Bearpark, J. J. Heyd, E. N. Brothers, K. N. Kudin, V. N. Staroverov, T. A. Keith, R. Kobayashi, J. Normand, K. Raghavachari, A. P. Rendell, J. C. Burant, S. S. Iyengar, J. Tomasi, M. Cossi, J. M. Millam, M. Klene, C. Adamo, R. Cammi, J. W. Ochterski, R. L. Martin, K. Morokuma, O. Farkas, J. B. Foresman, and D. J. Fox, Gaussian, Inc., Wallingford CT, 2016.
10. (a) R. L. Martin, *J. Chem. Phys.*, 2003, **118**, 4775-4777; (b) E. R. Batista and R. L. Martin, *J. Phys. Chem. A*, 2005, **109**, 3128-3133; (c) E. R. Batista and R. L. Martin, *J. Phys. Chem. A*, 2005, **109**, 9856-9859; (d) L.E. Roy, G. Scalmani, R. Kobayashi and E.R. Batista, *Dalton Trans.*, 2009, 6719-6721.